LETTER

Emergence of a resistance anomaly by Cu-doping in TaSe$_3$

To cite this article: A. Nomura *et al* 2017 *EPL* **119** 17005

View the article online for updates and enhancements.

Related content

- Pressure-induced enhancement in the superconductivity of ZrTe3
  Kemin Gu, Resta A Susilo, Feng Ke et al.

- The effect of pressure on the charge-density wave and superconductivity inZrTe3
  K Yamaya, M Yoneda, S Yasuzuka et al.

- Raising Tc in charge density wave superconductor ZrTe3 by Ni intercalation
  Hechang Lei, Xiangde Zhu and C. Petrovic

Recent citations

- Effect of Cu doping on superconductivity in TaSe$_3$: Relationship between superconductivity and induced charge density wave
  A. Nomura *et al*

Emergence of a resistance anomaly by Cu-doping in TaSe₃

A. Nomura[1], K. Yamaya[2], S. Takayanagi[2], K. Ichimura[1,2], T. Matsuura[3] and S. Tanda[1,2]

[1] *Department of Applied Physics, Hokkaido University - Sapporo 060-8628, Japan*
[2] *Center of Education and Research for Topological Science and Technology, Hokkaido University Sapporo 060-8628, Japan*
[3] *Department of Electrical and Electronic Engineering, National Institute of Technology, Fukui College Sabae, 916-8507, Japan*

Abstract – We have synthesized single crystals doped with Cu atoms in TaSe₃ which exhibits no Charge Density Wave (CDW) transition, and measured precisely the temperature dependence of the resistance. We discover an anomalous sharp dip in the temperature derivative of the resistance (dR/dT) at about 91 K in Cu-doped TaSe₃, which is never observed in pure TaSe₃. The dip suggests that there is a phase transition with a relative increase in resistance. In addition, the dip is "γ" shaped. We reveal that the same "γ"-shaped dip in dR/dT is commonly observed at the CDW transition temperature in many CDW conductors, which is a universal consequence resulting from the opening and growth of a CDW gap on a Fermi surface. Furthermore, the result of the single-crystal X-ray diffraction (XRD) analysis implies that Cu-doping increases the lattice parameter of the a-axis and c-axis and decreases that of the b-axis, leading to an improvement in the nesting condition. Based on the "γ"-shaped dip and the result of the single-crystal XRD analysis, we conclude that a CDW emerges by Cu-doping in TaSe₃.

Introduction. – The induction of superconductivity has helped in the search for new superconducting characteristics and in answering unresolved questions about superconductivity. For example, high-temperature superconductivity has been induced by doping carriers in insulators [1]. As a result, a new superconductivity mechanism was found, and the transition temperature (T_C) achieved 164 K under high pressure [2]. In addition, it was found that conventional superconductivity appears in a sulfur hydride system under high pressure [3]. This discovery brought the leap of T_C to 203 K and showed the possibility of realizing a higher T_C in other hydrogen-based materials. Moreover, superconductivity was induced in some Charge Density Wave (CDW) compounds by employing doping or high pressure, and the coexistence or competition of induced superconductivity with CDW was investigated [4–9]. Thus, the induction of superconductivity provides many opportunities to study superconductivity.

CDW is a macroscopic quantum state as well as superconductivity. CDWs occur in low-dimensional metals as the result of the Peierls instability of Fermi surface. Previous CDW studies have provided a lot of knowledge about the mechanisms and the dynamics of CDW

by targeting materials with intrinsic CDW states [10,11]. However, the next stage of this research should involve inducing a CDW in materials that do not normally exhibit one, because new CDW characteristics might be obtained and it will provide many opportunities to deal with unresolved issues as well as superconductivity. For example, new driving mechanisms other than conventional Fermi surface nesting might be found as reported for NbSe₂ [12] and TiSe₂ [13]. Moreover, if a CDW is induced in materials that exhibit superconductivity, we can study the relationship between induced CDW and superconductivity and compare it with the conventional coexistence or competition.

TaSe₃ is a predominant candidate material capable of inducing a CDW. TaSe₃ is one of the transition metal trichalcogenides, MX₃ (M: Nb, Ta; X: S, Se). MX₃ are quasi–one-dimensional conductors with chain structures, in which electric currents are passed well in the direction of the chain axis. Generally, the Fermi surface of a quasi–one-dimensional conductor is close to a plane. If the Fermi surface was translated by a wave vector, it would overlap well with that before translation, *i.e.*, the nesting condition is good. This indicates the intrinsic instability

Table 1: The synthesis condition and result of ICP-AES.

Crystal	Nominal value of Cu (x)	Growth temperature	Ratio of amount of substance		
			Ta	Se	Cu
Pure TaSe$_3$	0	678 °C	1	2.79 ± 0.10	0
Cu-doped TaSe$_3$	0.0075	678 °C	1	2.86 ± 0.10	0.0051 ± 0.0010
Cu-doped TaSe$_3$	0.05	678 °C	1	2.91 ± 0.10	0.0095 ± 0.0010
Cu-doped TaSe$_3$	0.05	708 °C	1	2.89 ± 0.10	0.0112 ± 0.0010

of the Fermi surface, and as a result, a CDW develops below the transition temperature in a quasi–one-dimensional conductor. In fact, CDW transitions are observed in NbSe$_3$, TaS$_3$, and NbS$_3$ [14–16]. On the other hand, TaSe$_3$ exhibits no CDW transition over the entire temperature range, but the superconductivity transition occurs at about 2 K although it is a quasi–one-dimensional conductor [17,18]. It is considered that the irregular behavior arises because TaSe$_3$ is more three-dimensional than the other MX$_3$ compounds. Actually, the electrical conductivity anisotropy ($\sigma_\parallel / \sigma_\perp$) of TaSe$_3$ is 3–15, while that of TaS$_3$ is $\sim$100 and that of NbSe$_3$ is 10–20 [19–22]. Furthermore, according to the band calculation, TaSe$_3$ has two-dimensional Fermi surfaces, which are described as fused tunnels running in the ($-a^* + c^*$) direction in contrast to the one-dimensional flat Fermi surfaces of NbSe$_3$ and TaS$_3$ [23]. Conversely, if we can reduce the dimensionality, TaSe$_3$ may also exhibit a CDW.

There is impurity doping as a predominant candidate method capable of reducing the dimensionality in TaSe$_3$. In TaSe$_3$, the chains are weakly bonded by van der Waals forces. Therefore, if impurities are doped in TaSe$_3$, the impurities are expected to enter in the van der Waals gap and to increase the distance between chains. Actually, in the transition metal dichalcogenides, MX$_2$ (M: Ti, Nb, Ta; X: S, Se), where MX$_2$ layers are weakly bonded by van der Waals forces, impurities enter between layers and increase the distance between layers, as reported for Cu$_x$TiSe$_2$ [5,24]. If Cu-doping increases the distance between chains in TaSe$_3$ as well as Cu$_x$TiSe$_2$, the overlap between electron wave functions perpendicular to the chain axis decreases, leading to an increase in electrical conductivity anisotropy. As a result, the dimensionality may be reduced.

In our research, we tried to induce a CDW in TaSe$_3$ by Cu-doping, and investigated the presence of a CDW by measuring the resistance as a function of temperature.

Experimental. – We prepared single crystals of pure TaSe$_3$ and Cu-doped TaSe$_3$ synthesized by the vapor phase transport method. We obtained three kinds of Cu-doped TaSe$_3$ crystals by changing the nominal value of Cu (x) and the growth temperature. First, Ta, Se and Cu materials (99.95%, 99.999%, and 99.9% respectively, Nilaco Corp.) were sealed with a molar ratio of 1 to 3 to x ($x = 0$, 0.0075, and 0.05) in evacuated quartz tubes. They were then heated at 678 °C ($x = 0$, 0.0075, and 0.05) and

708 °C ($x = 0.05$), and maintained at the temperature for about seven days. Finally, the tubes were quenched in water. In this way, we obtained whisker crystals with a typical dimension of $5\,\mu\text{m} \times 10\,\mu\text{m} \times 5\,\text{mm}$.

To examine the actual concentration of Cu in the crystals, we performed inductively coupled plasma atomic emission spectroscopy (ICP-AES) using an ICPE-9000 (Shimadzu Corp.). We determined the average Cu concentration for a bundle of the whisker crystals (a few milligrams).

The crystal structure was examined by single-crystal X-ray diffraction (XRD) analysis with Cu $K\alpha$ radiation ($\lambda = 1.5418\,\text{Å}$) using a Rigaku XtaLAB P200 diffractometer. The lattice parameters were extracted by fitting the XRD spectra using CrysAlisPro.

The temperature dependence of the resistance along the b-axis (parallel to the chain axis) was precisely measured with a dc four-probe measurement. We measured the temperature dependence of the resistance, while the samples were warmed from 4.2 to 280 K for about 30 hours. The temperature was measured with a Cernox resistance sensor.

Results. – The synthesis condition and the result of ICP-AES are listed in table 1. From the ratio of the amount of substance determined by ICP-AES, we define the Cu concentration as the ratio of Cu to Ta given as a percentage. The Cu concentrations of the Cu-doped TaSe$_3$ were 0.51 ± 0.10%, 0.95 ± 0.10% and 1.12 ± 0.10%. Thus, together with pure TaSe$_3$, we prepared four kinds of crystals with different Cu concentrations. The Cu concentration did not exceed 1.2% even when the nominal value for Cu was more than 5%.

Figure 1 shows the lattice parameters determined by single-crystal XRD analysis as a function of Cu concentration. The crystal structure of TaSe$_3$ is monoclinic. The a-axis and c-axis are perpendicular to the b-axis, which is the direction of the chain axis, and β is the angle between the a-axis and the c-axis. The lattice parameters obtained for three samples of pure TaSe$_3$ were $a = 10.402$–$10.409\,\text{Å}$, $b = 3.498$–$3.500\,\text{Å}$, $c = 9.824$–$9.828\,\text{Å}$ and $\beta = 106.24$–$106.27°$, which showed little sample dependence. However, the obtained values were in good agreement with previously reported values of $a = 10.402 \pm 0.004\,\text{Å}$, $b = 3.495 \pm 0.002\,\text{Å}$, $c = 9.829 \pm 0.004\,\text{Å}$, $\beta = 106.26 \pm 0.03°$ [25], and $a = 10.374\,\text{Å}$, $b = 3.501\,\text{Å}$, $c = 9.827\,\text{Å}$, $\beta = 106.11°$ [26]. The lattice parameters we
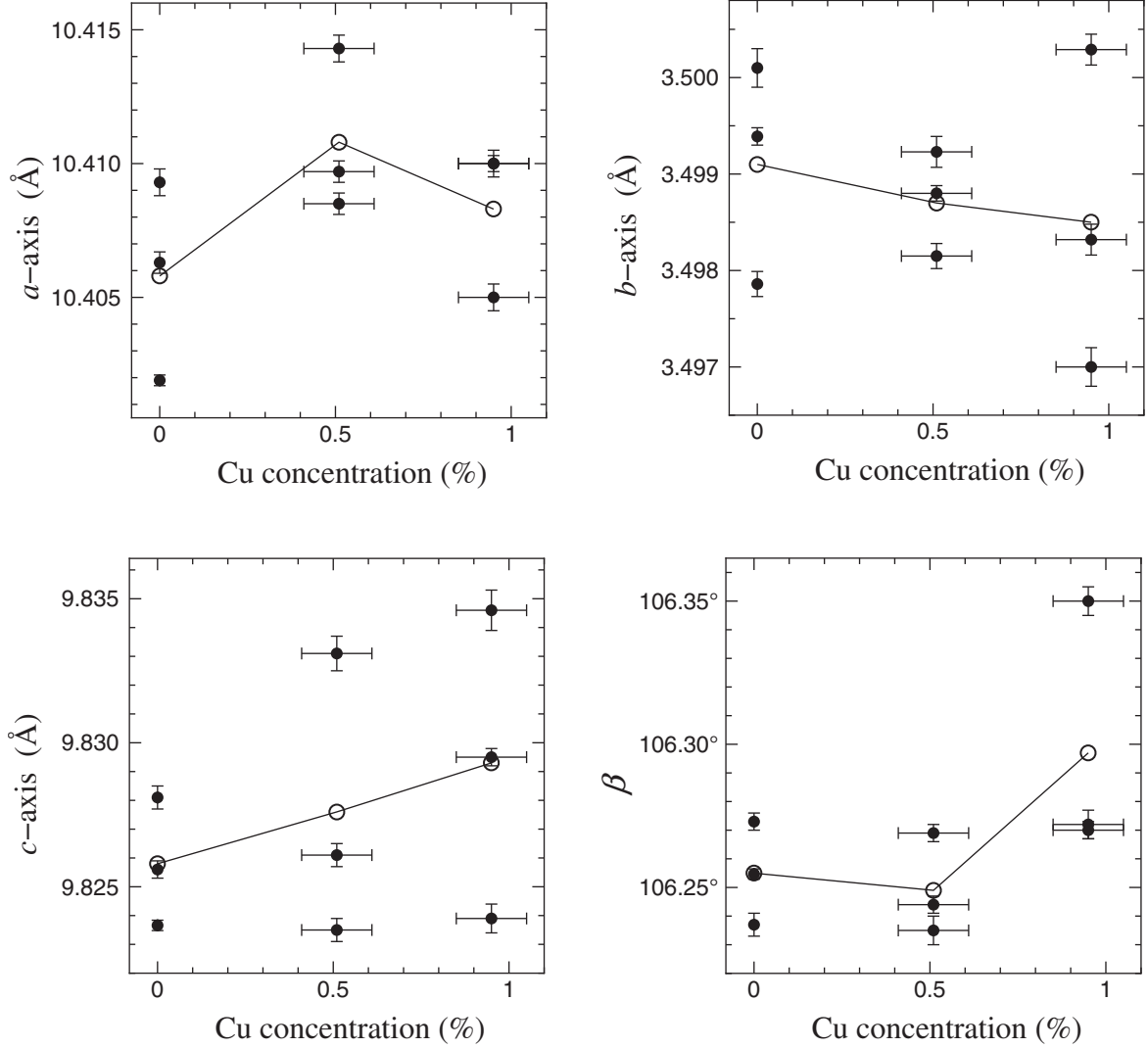
Fig. 1: The lattice parameters of pure TaSe$_3$ and Cu-doped TaSe$_3$ determined by single-crystal XRD analysis. Three samples for each Cu concentration are measured. The filled circles show the data for each sample, and the open circles show the average value for each Cu concentration.

obtained for three samples of each Cu-doped TaSe$_3$ also exhibited sample dependence in almost the same range as that of pure TaSe$_3$. The Cu concentration dependence of lattice parameters does not show a clear change which satisfies Vegard's law. However, the average values for the a-axis, c-axis and β tended to increase slightly as the Cu concentration increased, while that of the b-axis tended to decrease slightly.

The temperature dependence of the resistance was measured for several samples for each Cu concentration. Figure 2 shows typical data for pure TaSe$_3$ and Cu-doped TaSe$_3$. In all the samples, as the temperature increased, the resistance monotonically increased with a convex downward curvature in the low-temperature range ($T < 70$ K) and with a convex upward curvature in the high-temperature range ($T > 70$ K) unlike the linear R-T curve for typical metals. The residual resistance ratios ($RRR = R(280\,\text{K})/R(4.5\,\text{K})$) were 43.2–57.1

in pure TaSe$_3$, 5.3–6.3 in Cu-doped TaSe$_3$ (0.51%), 3.2–3.5 in Cu-doped TaSe$_3$ (0.95%) and 3.0–3.3 in Cu-doped TaSe$_3$ (1.12%). The RRR decreased with increasing Cu concentration.

Figure 3(a) shows the temperature dependence of the resistance normalized by the difference between the resistance at 4.5 K and that at 280 K to compare the temperature-dependent parts of the resistance of pure TaSe$_3$ and Cu-doped TaSe$_3$. The temperature dependence of the resistance shows almost the same functional form for all samples. As the Cu concentration increased, the normalized resistance at 4.5 K increased almost as a linear function of the Cu concentration as shown in fig. 3(b). Therefore, Matthiessen's rule holds for the Cu-doped TaSe$_3$ system.

To compare these temperature dependences of the resistance in detail, we plot the temperature derivative of the resistance ($\mathrm{d}R/\mathrm{d}T$) in fig. 3(c). In pure TaSe$_3$, the $\mathrm{d}R/\mathrm{d}T$
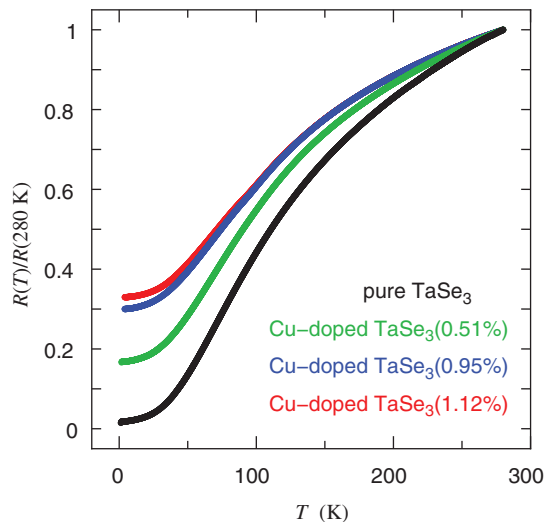
Fig. 2: (Colour online) The temperature dependence of the resistance normalized by the resistance at 280 K of pure TaSe$_3$ and Cu-doped TaSe$_3$.

increased monotonically from 4.5 K, showed a maximum of 70 K, and decreased monotonically above 70 K. In all Cu-doped TaSe$_3$ with different Cu concentrations, the dR/dT showed a similar temperature dependence to that of pure TaSe$_3$ over almost the entire temperature range. However, there was an anomalous sharp dip in the dR/dT at about 91 K in Cu-doped TaSe$_3$, but never in pure TaSe$_3$. In Cu-doped TaSe$_3$ (1.12%) with the maximum Cu concentration, the dR/dT suddenly decreased from about 102 K to about 91 K, showed a narrow minimum, and began to increase at about 91 K. Below about 91 K, it gradually returned to a temperature dependence similar to that of pure TaSe$_3$. In summary, the anomalous sharp dip was "γ" shaped. The depth of the dip increased with increasing Cu concentration. We call the temperature at which the dR/dT drops most the dip appearance temperature, T_{dip}. The T_{dip} was observed as 92 ± 2 K and 91 ± 2 K for Cu concentrations of 0.95% and 1.12%, respectively. There was no significant difference between the T_{dip} values of Cu-doped TaSe$_3$ (0.95%) and Cu-doped TaSe$_3$ (1.12%) beyond the measurement accuracy (± 2 K). In Cu-doped TaSe$_3$ (0.51%), the dip was too small to define the minimum dR/dT. The dip was reproduced in all samples measured for the same Cu concentration. Furthermore, the same T_{dip} was observed by cooling and heating the Cu-doped TaSe$_3$ (1.12%) sample using another mesurement instrument, that is, no thermal hysteresis is observed.

Discussion. – The single-crystal XRD analysis shows that the lattice parameters have sample dependence and do not show Vegard's law clearly for increasing Cu concentration, as shown in fig. 1. On the other hand, the RRR and the depth of the dip change systematically as the Cu concentration increases (see figs. 2 and 3(c)). The beam diameter used in the single-crystal XRD analysis is
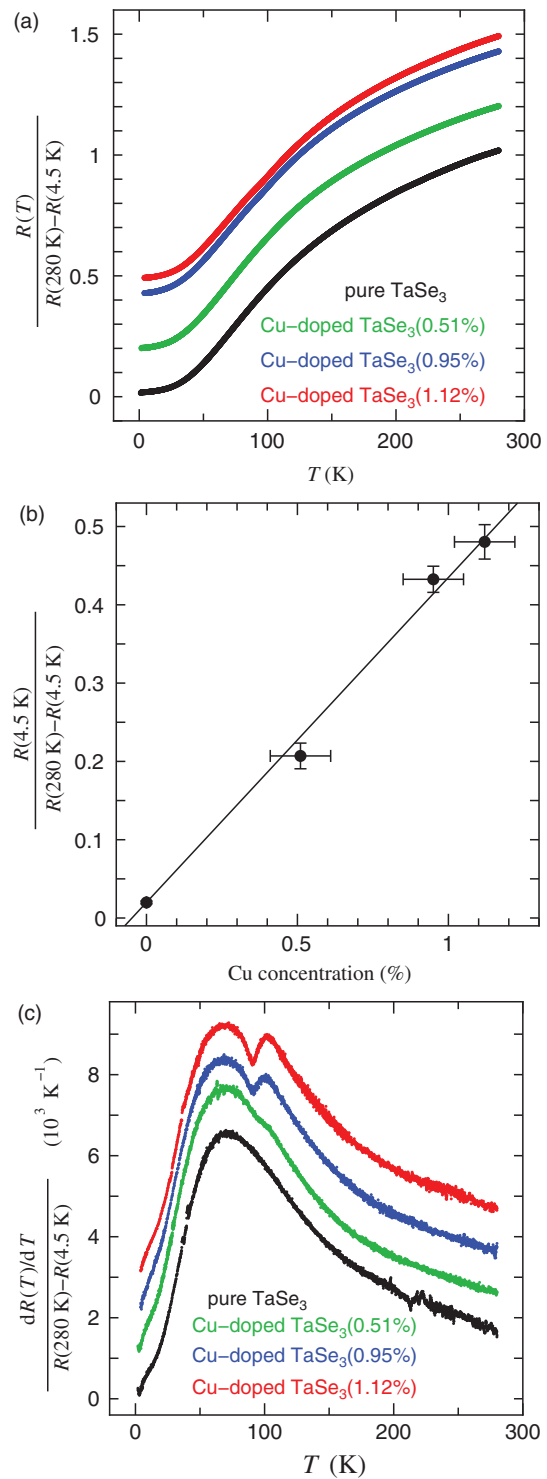

Fig. 3: (Colour online) (a) The temperature dependence of the resistance normalized by the difference between the resistance at 4.5 K and that at 280 K of pure TaSe$_3$ and Cu-doped TaSe$_3$. (b) The resistance at 4.5 K normalized by the difference between the resistance at 4.5 K and that at 280 K as a function of Cu concentration. The average value is shown for each Cu concentration. (c) The temperature derivative of the normalized resistance in panel (a). The curves of Cu-doped TaSe$_3$ (0.51%), Cu-doped TaSe$_3$ (0.95%) and Cu-doped TaSe$_3$ (1.12%) are shifted vertically by 0.001, 0.002 and 0.003 K^{-1}, respectively.

0.15 mm and, as a result, the lattice parameters are determined as the average value over a local region of 0.15 mm in comparison with the resistance that is obtained as the average value over the region of 1–3 mm between the voltage terminals. Thus, the inhomogeneity in a single crystal may cause the sample dependence of the lattice parameters. However, the inhomogeneous distribution of Cu atoms is not the main cause because the sample dependence is observed not only in Cu-doped TaSe$_3$ but also in pure TaSe$_3$. The ideal value of the molar ratio of Se to Ta is 3. However, the actual molar ratio obtained using ICP-AES is 2.8–2.9 as shown in table 1. This fact shows excess Ta atoms or Se vacancies. It is possible that there is inhomogeneous distribution of Ta and Se atoms in a single crystal which disturbs the lattice parameters and obscures the effect of Cu-doping, *i.e.*, Vegard's law.

Therefore, we focus on the average value of the lattice parameter for each Cu concentration and discuss the change in lattice parameters by Cu-doping. As shown in fig. 1, the average lattice parameter value tends to increase on the a-axis and c-axis (perpendicular to the chain axis) and tends to decrease on the b-axis (parallel to the chain axis) as the Cu concentration increases. The expansion of the a-axis and c-axis indicates that Cu atoms may be intercalated in the van der Waals gap between chains. When the distance between chains is increased, and the chain axis is contracted, the dimensionality is expected to decrease because the overlap between wave functions perpendicular to the chain axis decreases and that in the chain axis direction increases. Therefore, the result of the single-crystal XRD analysis implies that the change in lattice parameters caused by Cu-doping changes the Fermi surfaces from two-dimensional tunnel-like to one-dimensional flat. This would lead to a better nesting condition in Cu-doped TaSe$_3$ than in pure TaSe$_3$.

In addition, we can consider the number of carriers to be another physical quantity that is changed by Cu-doping. It is reported that the Cu atoms intercalated in the van der Waals gap are donors contributing delocalized electrons at the Fermi level [24]. The Cu atoms in Cu-doped TaSe$_3$ are assumed to be intercalated in van der Waals gaps, and contribute delocalized electrons. TaSe$_3$ is a semimetal with several Fermi surfaces which consist of a hole and an electron band [23]. In addition, the result of angle-resolved photoemission spectroscopy (ARPES) exhibits a high density of states near the Fermi level [20]. Thus, the density of states at the Fermi energy and the form of the Fermi surfaces are sensitive to a change in the number of carriers. It is possible that the change in the number of carriers caused by Cu-doping can also change the nesting condition although it does not necessarily get better.

We find an anomalous sharp dip in the dR/dT value in the temperature dependence of the dR/dT of Cu-doped TaSe$_3$, which is never observed in that of pure TaSe$_3$, as shown in fig. 3(c). The dip in dR/dT is "γ" shaped with a sudden decrease and a narrow minimum. Thus, the dip suggests a sudden change in state, namely a phase

transition. The emergence of a structural transition is suggested in pure TaSe$_3$ under uniaxial strain [27]. However, the phase transition in Cu-doped TaSe$_3$ would not be a first-order transition because we observe no thermal hysteresis.

We discuss how the resistance changes in the vicinity of the phase transition temperature where a dip in dR/dT is present in Cu-doped TaSe$_3$. When the dR/dT drops, the decrease in resistance caused by the decrease in temperature is suppressed. Thus, the resistance below the onset temperature of the dip (102 K) is larger than the resistance extrapolated from the resistance-temperature curve above 102 K assuming that there is no dip in dR/dT. In summary, the dip in dR/dT means a relative increase in resistance. MX$_3$ compounds (NbSe$_3$, TaS$_3$, NbS$_3$) other than TaSe$_3$ show anomalous increases in resistance at the CDW transition temperatures (T_{CDW}) because the whole or part of the Fermi surfaces disappears and the number of carriers decreases [14–16]. Therefore, the phase transition with an increase in resistance in Cu-doped TaSe$_3$ is most likely to be a CDW transition although the resistance increase is relative.

We discuss the "γ"-shaped dip discovered in Cu-doped TaSe$_3$ by comparison with the temperature dependence of the dR/dT in CDW conductors such as NbSe$_3$ [28], DyTe$_3$ [29] and ZrTe$_3$ [30]. These CDW conductors show the metallic temperature dependence of the resistance in the normal state above the T_{CDW}, and the resistance increase at the T_{CDW}. However, the temperature dependence of the resistance shows metallic behavior again at lower temperatures because the Fermi surfaces partly remain due to imperfect nesting. Although the magnitude of the resistance increase at T_{CDW} is different for the three CDW conductors, we find out a common dip in the dR/dT value corresponding to the resistance increase. The dR/dT is constant above the T_{CDW}, however with decreasing temperature, it falls sharply at the T_{CDW} and then starts to increase at the minimum point. At lower temperatures, it increases more gradually with a convex upward curvature and approaches a certain value. In short, the temperature dependence of the dR/dT shows the common "γ"-shaped dip, indicating the universal law peculiar to the CDW transition. The law states that a CDW is formed with an energy gap opening on a Fermi surface. In the BCS theory on the CDW transition, the energy gap opens at T_{CDW} and grows obeying the temperature dependence of the gap function. The opening and growth of the CDW gap reduce the number of conducting carriers with decreasing temperature, leading to an increase in resistance near T_{CDW}, and at the same time the dR/dT has a "γ"-shaped dip. This fact strongly indicates that the "γ"-shaped dip observed in Cu-doped TaSe$_3$ is caused by the CDW transition.

As shown in fig. 3(c), the T_{dip} of Cu-doped TaSe$_3$ is about 91 K, which is lower than the T_{CDW} of the other MX$_3$ compounds (340 K in NbS$_3$ [16], 218 K in TaS$_3$ [21], and 145 K in NbSe$_3$ [14]). Originally pure TaSe$_3$ has

two-dimensional Fermi surfaces [23], where the nesting condition is the worst in MX_3 compounds, thus it shows no CDW transition. Even if Fermi surfaces change and a CDW emerges in $TaSe_3$, the T_{CDW} is expected to be lower than the T_{CDW} of the other MX_3. Therefore, it will be consistent to assume that T_{dip} in Cu-doped $TaSe_3$ corresponds to T_{CDW}.

From the discussions above, the main features of the Cu-doped $TaSe_3$ system are summarized as follows: i) The change in the lattice parameters caused by Cu-doping may change the form of Fermi surfaces which leads to a better nesting condition. ii) The dip in dR/dT exhibits a characteristic of phase transition with a relative increase in resistance. iii) The dip in dR/dT is "γ" shaped and the same "γ"-shaped dip is commonly observed in many CDW conductors. Therefore, we can conclude that a CDW emerges by Cu-doping in $TaSe_3$.

If the dip in dR/dT in Cu-doped $TaSe_3$ is due to the CDW transition, the size of the dip, *i.e.*, the size of the relative resistance increase, corresponds to the ratio of the reduction of the Fermi surfaces due to the CDW transition. For example, in $NbSe_3$, two large humps with different sizes are observed in the temperature dependence of the resistance [31]. From the sizes of the two resistance increases, Kawabata estimates that about 30% of the Fermi surfaces disappears at the higher T_{CDW} and about 70% of the remainder disappears at the lower T_{CDW}. In the present case, even if the Cu concentration is 1.12%, the relative resistance increase in Cu-doped $TaSe_3$ is extremely small. This result indicates that the reduction ratio of the Fermi surfaces is very small and a large number of normal carriers remain at temperatures below the T_{CDW}. This result is also supported by the fact that Matthiessen's rule holds, as shown in fig. 3(a) and (b).

Here we discuss the relationship between the size of the resistance increase at T_{CDW} and the T_{CDW} value. When the CDW is suppressed by Cu-doping in $TiSe_2$ or by Se-doping in $ZrTe_3$, the size of the resistance increase becomes smaller as the doping concentration increases, and the T_{CDW} value also decreases [5,9]. These results are consistent with the prediction obtained for CDW with the mean-field theory, which shows a positive correlation between T_{CDW} and the area of the reduced Fermi surface, that is, the size of the resistance increase. As seen in fig. 3(c), in the Cu-doped $TaSe_3$ system, the size of the dip in dR/dT (the size of the relative resistance increase) increases with increasing Cu concentration, while we observe no clear change in T_{dip} for Cu-doped $TaSe_3$ (0.95%) and Cu-doped $TaSe_3$ (1.12%); here, T_{dip} corresponds to T_{CDW}. In other words, no clear change in T_{CDW} is observed with increasing Cu concentration within our T_{CDW} measurement accuracy (± 2 K). A comparison of our result to $Cu_x TiSe_2$ and $ZrTe_{3-x}Se_x$ shows that the change in T_{CDW} per $x = 0.0017$ (0.17% of doping concentration) is about 4 K in $Cu_x TiSe_2$ and about 3 K in $ZrTe_{3-x}Se_x$. These values are almost the same as our T_{CDW} measurement accuracy. It may be hard to detect the change in

T_{CDW} clearly because the change in the Cu concentration is very small (0.17%) in our study. Therefore, we can conclude that our result regarding the relationship between the size of the relative resistance increase and T_{CDW} does not contradict the positive correlation predicted from the mean-field theory.

The above discussions about the CDW transition are based on the scenario of the Fermi surface nesting. However, the resistance increase seen in Cu-doped $TaSe_3$ is extremely small, suggesting alternative scenario for the CDW formation. Rice and Scott propose that Fermi surfaces with saddle points can be unstable against CDW formation [32]. In this model, only a relatively small area of Fermi surfaces disappears and a large area of those remains. Furthermore, the saddle points act as scattering sinks in the high-temperature phase above T_{CDW} and the conductivity can be enhanced at the T_{CDW} by the disappearance of the saddle points. As a result, the resistance increase due to the CDW transition is suppressed. Therefore, the present result suggests the possibility that the CDW formation is driven by the mechanism of Rice and Scott. Although the presence of saddle points in pure $TaSe_3$ is not mentioned by the result of the band calculation [23], the result of ARPES shows that there is the flat band region with a high density of states near the Fermi level in pure $TaSe_3$ [20]. This singularity might drive the CDW transition in Cu-doped $TaSe_3$. In order to verify this mechanism, the band structure of Cu-doped $TaSe_3$ has to be investigated by ARPES.

Conclusion. – By measuring precisely the temperature dependence of the resistance in pure $TaSe_3$ and Cu-doped $TaSe_3$, we discovered an anomalous sharp dip in the temperature dependence of the temperature derivative of the resistance (dR/dT) in Cu-doped $TaSe_3$, which is never observed in pure $TaSe_3$. The dip suggests that there is a phase transition with a relative increase in resistance. Furthermore, the dip is "γ" shaped. We reveal that many CDW conductors commonly exhibit the same "γ"-shaped dip in dR/dT at the CDW transition temperature, which is a universal consequence of the opening and growth of a CDW gap on a Fermi surface. Furthermore, the result of the single-crystal X-ray diffraction (XRD) analysis implies that the lattice parameters perpendicular to the chain axis increase and that parallel to the chain axis decreases by Cu-doping, leading to an improvement in the nesting condition. From the "γ"-shaped dip and the result of the single-crystal XRD analysis, we conclude that a CDW emerges by Cu-doping in $TaSe_3$. Further studies are needed to obtain direct evidence of the CDW transition. In addition, we are studying the relationship between the emerging CDW and superconductivity, because $TaSe_3$ exhibits a superconductivity transition at about 2 K.

$$* * *$$

REFERENCES

[1] BEDNORZ J. G. and MÜLLER K. A., *Z. Phys. B - Condens. Matter*, **64** (1986) 189.

[2] GAO L., XUE Y. Y., CHEN F., XIONG Q., MENG R. L., RAMIREZ D., CHU C. W., EGGERT J. H. and MAO H. K., *Phys. Rev. B*, **50** (1994) 4260(R).

[3] DROZDOV A. P., EREMETS M. I., TROYAN I. A., KSENOFONTOV V. and SHYLIN S. I., *Nat. Phys.*, **525** (2015) 73.

[4] YASUZUKA S., MURATA K., FUJIMOTO T., SHIMOTORI M. and YAMAYA K., *J. Phys. Soc. Jpn.*, **74** (2005) 1782.

[5] MOROSAN E., ZANDBERGEN H. W., DENNIS B. S., BOS J. W. G., ONOSE Y., KLIMCZUK T., RAMIREZ A. P., ONG N. P. and CAVA R. J., *Nat. Phys.*, **2** (2006) 544.

[6] KUSMARTSEVA A. F., SIPOS B., BERGER H., FORRÓ L. and TUTIŠ E., *Phys. Rev. Lett.*, **103** (2009) 236401.

[7] SIPOS B., KUSMARTSEVA A. F., AKRAP A., BERGER H., FORRÓ L. and TUTIŠ E., *Nat. Mater.*, **7** (2008) 960.

[8] LI L. J., LU W. J., ZHU X. D., LING L. S., QU Z. and SUN Y. P., *EPL*, **97** (2012) 67005.

[9] ZHU X., NING W., LI L., LING L., ZHANG R., ZHANG J., WANG K., LIU Y., PI L., MA Y., DU H., TIAN M., SUN Y., PETROVIC C. and ZHANG Y., *Sci. Rep.*, **6** (2016) 26974.

[10] MONCEAU P., *Adv. Phys.*, **61** (2012) 325.

[11] MONCEAU P., *Physica B*, **460** (2015) 2.

[12] VALLA T., FEDOROV A. V., JOHNSON P. D., GLANS P-A., MCGUINNESS C., SMITH K. E., ANDREI E. Y. and BERGER H., *Phys. Rev. Lett.*, **92** (2004) 086401.

[13] SUGAWARA K., NAKATA Y., SHIMIZU R., HAN P., HITOSUGI T., SATO T. and TAKAHASHI T., *ACS Nano*, **10** (2016) 1341.

[14] ONG N. P. and MONCEAU P., *Phys. Rev. B*, **16** (1977) 3443.

[15] SAMBONGI T., TSUTSUMI K., SHIOZAKI Y., YAMAMOTO M., YAMAYA K. and ABE Y., *Solid State Commun.*, **22** (1977) 729.

[16] WANG Z. Z., MONCEAU P., SALVA H., ROUCAU C., GUEMAS L. and MEERSCHAUT A., *Phys. Rev. B*, **40** (1989) 11589.

[17] REGUEIRO M. N., *Solid State Commun.*, **60** (1986) 797.

[18] SAMBONGI T., YAMAMOTO M., TSUTSUMI K., SHIOZAKI Y., YAMAYA K. and ABE Y., *J. Phys. Soc. Jpn.*, **42** (1977) 1421.

[19] GESERICH H. P., SCHEIBER G., LÉVY F. and MONCEAU P., *Physica B*, **143** (1986) 174.

[20] PERUCCHI A., SØNDERGAARD C., MITROVIC S., GRIONI M., BARISIC N., BERGER H., FORRÓ L. and DEGIORGI L., *Eur. Phys. J. B*, **39** (2004) 433.

[21] TAKOSHIMA T., IDO M., TSUTSUMI K., SAMBONGI T., HONMA S., YAMAYA K. and ABE Y., *Solid State Commun.*, **35** (1980) 911.

[22] ONG N. P. and BRILL J. W., *Phys. Rev. B*, **18** (1978) 5265.

[23] CANADELL E., RACHIDI I. E.-I., POUGET J. P., GRESSIER P., MEERSCHAUT A., ROUXEL J., JUNG D., EVAIN M. and WHANGBO M.-H., *Inorg. Chem.*, **29** (1990) 1401.

[24] NOVELLO A. M., SPERA M., SCARFATO A., UBALDINI A., GIANNINI E., BOWLER D. R. and RENNER CH., *Phys. Rev. Lett.*, **118** (2017) 017002.

[25] BJERKELUND E., FERMOR J. H. and KJEKSHUS A., *Acta Chem. Scand.*, **20** (1966) 1836.

[26] YAMAYA K. and OOMI G., *J. Phys. Soc. Jpn.*, **51** (1982) 3512.

[27] TRITT T. M., STILLWELL E. P. and SKOVE M. J., *Phys. Rev. B*, **34** (1986) 6799.

[28] TSUNETA T., PhD Thesis, Hokkaido University (2004).

[29] SINCHENKO A. A., LEJAY P. and MONCEAU P., *Phys. Rev. B*, **85** (2012) 241104(R).

[30] TAKAHASHI S., SAMBONGI T., BRILL J. W. and ROARK W., *Solid State Commun.*, **49** (1984) 1031.

[31] KAWABATA K., *J. Phys. Soc. Jpn.*, **54** (1985) 762.

[32] RICE T. M. and SCOTT G. K., *Phys. Rev. Lett.*, **35** (1975) 120.